

Dynamical Regimes of Directional Viscous Fingering: Spatiotemporal Chaos and Wave Propagation

M. Rabaud, S. Michalland, and Y. Couder

Laboratoire de Physique Statistique, Ecole Normale Supérieure, 24 rue Lhomond, 75231 Paris CEDEX 05, France

(Received 31 July 1989)

In the opening gap between two moving surfaces, the interface between air and a viscous fluid can form a linear pattern of regular cells analogous to those of directional solidification. Depending on the values of the surface velocities, this pattern destabilizes in different ways. One regime presents the main characteristics of spatiotemporal intermittency of the type observed in the Kuramoto-Sivashinsky model. In the other, the cells become a propagative structure. Near one of the thresholds they show up as solitary waves; above, they form traveling domains of increasing size.

PACS numbers: 47.20.Hw, 47.20.Ky, 47.25.Ae, 68.10.La

The nonlinear spatiotemporal behavior of extended systems is generally complex because of the large number of degrees of freedom involved. Recent theoretical effort in this field has concentrated on ideal situations in which a one-dimensional system has an underlying basic periodic cellular state. Situations of this type can be described in the formalism of either amplitude or phase equations reviewed in Refs. 1 and 2. Two points have been particularly investigated: the transition of such systems to chaos and the possibility of obtaining propagative structures. The first aspect was initially investigated numerically on a model phase equation introduced by Kuramoto and Sivashinsky³ (KS) [and on its variant the Kolmogorov-Spiegel-Sivashinsky⁴ equation (KSS)]. It led to the characterization of a specific behavior: the spatiotemporal intermittency. Among the experiments on chaos in extended systems,⁵⁻⁸ it is only in the cases where the system is confined in one direction⁵ that this behavior is observed. A second possible dynamics in extended systems, the existence of propagative modes, was first observed experimentally in electroconvection⁸ and in binary-fluid-mixture convection,⁶ and was at the origin of important theoretical efforts.^{1,2}

We present an experiment in which the unstable one-dimensional medium is a linear front affected by what we will call *directional viscous fingering*. The similarity between crystal growth and viscous fingering⁹ led us to seek an experimental equivalent to directional solidification¹⁰ in viscous fingering. This meant that the Saffman-Taylor unstable front between two fluids of different viscosities had to be submitted to a stabilizing gradient localized in the laboratory frame of reference. This is in fact realized in several classical experiments on the interface between a viscous and a nonviscous fluid in the widening gap between a roller and a plane,¹¹ between two rollers,¹² in the narrow passages of journal bearings,¹³ and in the peeling of an adhesive tape.¹⁴ In a previous work¹⁵ we showed that the unstable front does have a dynamical behavior comparable to that of directional solidification and that its ruling equations are similar. We will show here that, if the two solid surfaces have independent velocities, a rich phenomenology of

nonlinear phenomena is obtained. Thus the same experiment lends itself to the study of several dynamical behaviors of one-dimensional extended systems.

The cell was formed by a hollow horizontal Plexiglas cylinder of inner radius $R_2=71$ mm and length $L_2=210$ mm and a smaller cylinder of radius $R_1=49$ mm ($L_1=200$ mm) off-centered inside it. The two axes were parallel to each other and placed so that only a very narrow gap separated the cylinders along one of their generatrix at the bottom of the apparatus. Two micrometers allowed the possibility of adjusting the minimum width of this gap b_0 ($100 \mu\text{m} < b_0 < 1$ mm) with a resolution of $15 \mu\text{m}$. The geometrical aspect ratio $\Gamma=L_1/b_0$ ranged between 200 and 2000 and gave patterns with up to 200 cells. The two cylinders were driven in rotation independently by two locked-in motors. The tangential velocities V_1 and V_2 of the inner and outer cylinders were defined with a resolution of 1 mm/s. A small amount of oil was introduced between the cylinders. This quantity was not a critical parameter as long as it was chosen small enough to avoid a gravity effect and large enough to fill the minimum gap b_0 . We used a silicon oil, Rhodorsyl 47V100, with dynamical viscosity $\mu=96.5 \times 10^{-3}$ kg/ms and surface tension $T=20.9 \times 10^{-3}$ N/m at 25°C. This oil insured a good wetting of the Plexiglas surfaces. We observed the interfaces from below, through the external roller. The front shape was recorded on videotape. In order to visualize the spatiotemporal evolution of the front we could select one single video sweep line intersecting the cells and record its evolution as a function of time. A new video image was generated with 512 such lines separated by a tunable time delay.

The instability is due to the two surfaces moving away from each other: For each sign of V_1+V_2 one of the menisci is stable and the other can be unstable. We limit ourselves to the study of one meniscus ($V_1+V_2 > 0$). Roughly by increasing V_1+V_2 a threshold is met where the linear front destabilizes. On the entire stability limit drawn in Fig. 1 this is a supercritical process in which the front becomes a sinusoid of wavelength λ_c . Using the lubrication approximation, we previously analyzed¹⁵ the basic phenomena in the particular case where only

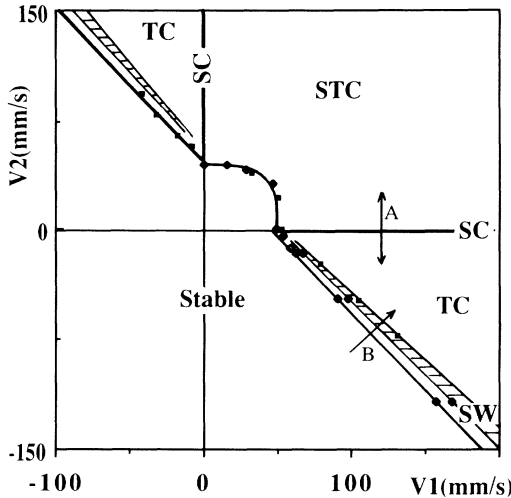


FIG. 1. Stability diagram of one meniscus in the plane (V_1, V_2) in a cell of minimum thickness $b_0 = 0.37$ mm. We observe stationary periodic cells (SC on the two axes), spatiotemporal chaos (STC), traveling cells (TC), and solitary waves (SW) moving on a stationary sinusoidal front (hatched region).

one cylinder is rotating and gave reasonable predictions for the values of V_c and λ_c . However, this treatment suggested that the state of the front would practically depend on $V_1 + V_2$ only. This is not what is observed experimentally. The onset values and the nonlinear behavior show that V_1 and V_2 form two independent control parameters. We will therefore describe (Fig. 1) the different regions of instability in the plane (V_1, V_2) . The threshold for counterrotating cylinders is fitted by $V_1 + V_2 = V_c$ ($V_c \approx 47$ mm/s for $b_0 = 0.37$ mm), but for corotating cylinders (V_1 and $V_2 > 0$) the front remains stable up to larger values of the mean rotation (Fig. 1). The further nonlinear evolution for larger values of V_1 and V_2 is different in different regions of the diagram. We can first remark that the same states of this front are obtained at points symmetrical with respect to the first bisector ($V_1 = V_2$). This shows that there is no influence of centrifugal forces (the Taylor number is very small), nor of the curvature of the cell. The simplest evolution, described in Ref. 15, is observed when only one cylinder is rotating, say the inner cylinder. With an increase of the velocity the amplitude of the instability grows larger and the front departs from its sinusoidal shape. It forms a series of parallel fingers separated by thin oil walls¹⁶ [Fig. 2(a)] very similar to directional solidification cells. The wavelength λ of the pattern decreases rapidly as the velocity increases and then tends to saturate. At all the velocities that we investigated (up to 50 times the initial threshold) the pattern reaches a stable, regular state and no chaos is observed. For all velocity changes, the pattern adapts easily to take an optimum wavelength;¹⁷ new cells are created by tip splitting or cells disappear when pinched off. Provided the structure has time to evolve,

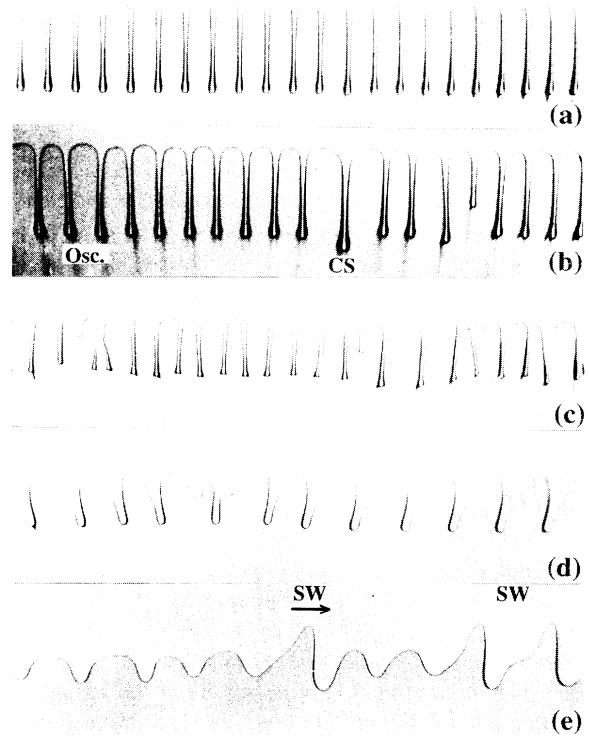


FIG. 2. In a cell with $b_0 = 0.37$ mm, photographs of a part of the front in the cases of (a) a stable pattern of stationary cells; (b) a pattern with weak spatiotemporal chaos showing a coherent structure (CS) and cells oscillating in time (Osc); (c) a pattern with strong spatiotemporal chaos; (d) a pattern of traveling waves, showing a source and a sink; and (e) solitary waves (SW) propagating on a stationary sinusoid.

there is no hysteresis. Specific transients are observed for small jumps of the velocity. The reorganization of the structure of initial wavelength λ occurs by a compression wave propagating along the front; one of the cells (usually near a boundary) adapts to the new shorter wavelength λ' , while its neighbor is first dilated, then shifts, and then stops and shrinks to λ' . The process repeats itself so that, transiently, the front is formed of a domain of shifting cells separating a region of wavelength λ' from a region of wavelength λ . The shifting cells and the boundaries of their domain propagate in opposite directions. These waves appear to be identical to those observed in liquid-crystal directional phase transition^{18(a)} and in eutectic growth^{18(b)} after a jump in the velocities.

When at point A (Fig. 1) a regular pattern has been created; two interesting dynamics are observed if the outer cylinder is now set in motion in one direction or the other.

(i) If the outer cylinder is set into corotation ($V_2 > 0$), defects appear in the linear array [Fig. 2(b)]: Constantly some cells split and others are pinched off. There ap-

pears to be no finite measurable threshold to this effect, which is observed even for very small V_2 . As V_2 is increased the disorder increases and ultimately the front is chaotic nearly everywhere [Fig. 2(c)]. The whole area labeled STC in Fig. 1 exhibits a spatiotemporal chaos. Along the front there is coexistence of chaotic domains (with strong fluctuations of the wavelength and constant formation and destruction of cells) with quiescent domains of steady, spatially periodic, cells. The difference between the two types of domains and their time evolution are very obvious after image processing (Fig. 3). The domains are not stable: They appear, extended, and then shrink and vanish, but for each value of the control parameter there is a mean fraction of the front occupied by chaotic domains. The system is thus chaotic with a spatiotemporal intermittency of the type observed in the KS and KSS models⁴ and in other types of experiments.⁵ A complete comparison of the experiment with the models would require both our showing that the elementary processes at work are the same and a statistical study of the domain sizes. An investigation of the latter is in progress and will be reported elsewhere. As our system offers the possibility, for weak chaos, of following in detail the individual defects and their relations, we will concentrate here on the former characterization. Experimentally when a cell is pinched off, it either creates other defects nearby, or else emits a phase wave which propagates along the front. This wave generates in the quies-

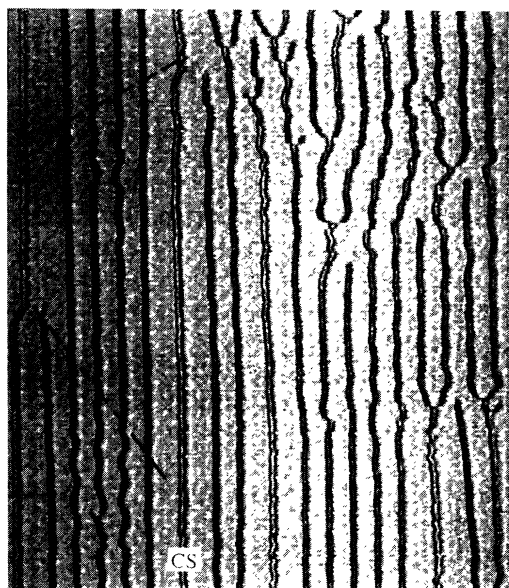


FIG. 3. Spatiotemporal evolution of a part of a front showing weak chaos (each horizontal line is a section of the front so that the dark lines show the positions of the oil films separating the cells) showing the stability of anomalous cells (CS), the coexistence of ordered and disordered regions, and a defect generating oscillations of the cells which propagate (dashed lines). The time elapsed from the top to the bottom is 20 s.

cent regions cell oscillations as shown in Fig. 2(b) in which a given cell swells and shrinks in opposite phase with its neighbors (optical mode). If the phase wave traveling along the front reaches an already slightly disturbed region, a chaotic burst appears in which cells are pinched off. So, chaotic domains are related through space and time by the waves. This process is that observed in simulations of the KS and KSS models.⁴ Another characteristic of the weak chaos of our fronts is the existence of coherent structures (CS) similar to those observed by Chaté and Maneville⁴ in the simulation of KSS equations. They are formed of two asymmetrical cells [Figs. 2(b) and 3] which occupy the width of three normal cells. These cells are transient in the strongly chaotic state but long lived near the threshold.

(ii) If, from A (Fig. 1), the outer cylinder is now set in counterrotation ($V_2 < 0$), the effect is also immediate. The cells become inclined relative to the front and begin to propagate [Fig. 2(d)]. Again we could not find a finite lower limit to the threshold. The velocity of translation of the cells is proportional to $(V_2)^{1/2}$. If V_2 is set abruptly, several domains of left- and right-traveling waves are formed, separated by sources and sinks. As time passes, annihilations of sources and sinks occur, increasing the size of the domains. Traveling cells are observed in all the regions labeled TC in Fig. 1. They are associated with a slow large-scale flow along the front; if one single source is present at the center, the fluid moves very slowly towards the extremity of the cylinders and accumulates there. Traveling cells have been observed in directional solidification but they are usually ascribed to the effect of the crystal anisotropy.¹⁰ In isotropic media, traveling waves are observed in convection in binary-fluid mixtures,⁶ electroconvection of liquid crystals,⁸ Taylor-Dean flow in partially filled cylinders,^{7(a)} and Taylor-Couette flows between counterrotating cylinders.^{7(b)} A theoretical model¹⁹ with coupled amplitude and phase equations exhibits a transition between motionless cells and traveling waves when parity is broken. As observed in the experiment, the wave velocity is then proportional to the square root of the distance to threshold.

We now want to characterize the lower limit of existence of TC. Moving away from point B of Fig. 1 by increasing V_1 and V_2 , we first cross the onset of the instability where a motionless sinusoidal front is formed. Then over a second, subcritical, threshold we begin to see recurrently the passage of a solitary wave (SW) moving in either direction along the front. These SW have a large, well determined, amplitude and a characteristic S shape [Fig. 2(e)]. They usually form during the splitting of a steady cell. Once formed, they travel, destroying locally the motionless sinusoid, which reappears behind. When two SW moving in opposite directions meet, they can cross each other, but more often one of them is destroyed. The spacing of these solitary waves decreases away from the onset and they can be generated by pack-

ets of several waves following each other.²⁰ As they become tightly packed, the front becomes entirely formed of traveling cells separated by sources and sinks [Fig. 2(d)]. Altogether there is in Fig. 1 a wedge-shaped region in which solitary waves coexist with a stationary sinusoid.

In conclusion, directional viscous fingering is an instability with a rich potential for the study of one-dimensional dynamics in extended systems. As it has two control parameters several different dynamical behaviors can be reached in the same experiment. We observed stable patterns and the waves that provide adaptation to an optimum wavelength, chaotic regimes with spatiotemporal intermittency, and traveling cells. The transition to this latter state is either supercritical (starting from *A*) or subcritical (starting from *B*). In the latter case it occurs through the spontaneous repeated formation of solitary waves, moving on the steady pattern.

We are very grateful to O. Cardoso for lending us an image-processing system he programmed and to H. Thomé for his design of the experimental cell. The authors have benefited from fruitful discussions with D. Bensimon, H. Chaté, P. Couillet, V. Croquette, V. Hakim, J. Lega, P. Maneville, and J. E. Wesfreid.

¹*Propagation in Systems far from Equilibrium*, edited by J. E. Wesfreid, H. R. Brand, P. Maneville, G. Albinet, and N. Boccara (Springer-Verlag, Berlin, 1984). Reviews on the dynamics of extended systems: A. C. Newell, *ibid.*, p. 122; H. R. Brand, *ibid.*, p. 206; P. Maneville, *ibid.*, p. 265.

²"New trends in Nonlinear Dynamics and Pattern Forming Phenomena: The Geometry of Nonequilibrium," edited by P. Couillet and P. Huerre (Plenum, New York, to be published).

³Y. Kuramoto, *Chemical Oscillations, Waves and Turbulence* (Springer-Verlag, Berlin, 1984); G. I. Sivashinsky, *Physica* (Amsterdam) **17D**, 243 (1985).

⁴H. Chaté and P. Maneville, *Phys. Rev. Lett.* **58**, 112 (1987); H. Chaté and B. Nicolaenko, in Ref. 2.

⁵S. Ciliberto and P. Bigazzi, *Phys. Rev. Lett.* **60**, 286 (1988); F. Daviaud, M. Dubois, and P. Bergé, *Europhys. Lett.* **9**, 441 (1989).

⁶(a) E. Moses, J. Fineberg, and V. Steinberg, *Phys. Rev.*

Lett. **61**, 838 (1988); (b) P. Kolodner and C. Surko, *Phys. Rev. Lett.* **61**, 842 (1988).

⁷(a) I. Mutabazi, J. J. Hegseth, C. D. Andereck, and J. E. Wesfreid, *Phys. Rev. A* **38**, 4752 (1988); (b) C. D. Andereck, S. S. Liu, and H. L. Swinney, *J. Fluid Mech.* **164**, 155 (1986).

⁸A. Joëts and R. Ribotta, *Phys. Rev. Lett.* **60**, 2164 (1988); I. Rehberg, S. Rasenat, and V. Steinberg, *Phys. Rev. Lett.* **62**, 756 (1989).

⁹Y. Couder, in Ref. 1; M. Rabaud, Y. Couder, and N. Gérard, *Phys. Rev. A* **37**, 935 (1988).

¹⁰R. Trivedi and K. Somboonsuk, *Acta Metall.* **33**, 1061 (1985); S. de Cheveigné, C. Guthmann, and M. M. Lebrun, *J. Phys. (Paris)* **47**, 2095 (1986).

¹¹J. R. A. Pearson, *J. Fluid Mech.* **7**, 481 (1960); M. D. Savage, *J. Fluid Mech.* **80**, 743 (1977); **80**, 757 (1977); **117**, 443 (1982).

¹²E. Pitts and J. Greiller, *J. Fluid Mech.* **11**, 33 (1961); C. C. Mill and G. R. South, *J. Fluid Mech.* **28**, 523 (1967); J. Greener, T. Sullivan, B. Turner, and S. Middleman, *Chem. Eng. Commun.* **5**, 73 (1980).

¹³G. I. Taylor, *J. Fluid Mech.* **16**, 595 (1963).

¹⁴A. D. McEwan and G. I. Taylor, *J. Fluid Mech.* **26**, 1 (1966).

¹⁵V. Hakim, M. Rabaud, H. Thomé, and Y. Couder, in Ref. 2.

¹⁶Beyond the front, the oil film left on the cylinder has a modulated thickness because the detachment of the walls creates periodic crests. This modulation is still present after one rotation and causes the other meniscus to be slightly wavy. We checked that this does not induce a feedback effect on the unstable front; collecting or spreading the oil film does not affect the unstable front.

¹⁷This is linked with the isotropy of the system; if periodic grooves are etched on one of the cylinders, the tip of the cells are pinned onto them. Beyond the velocity for which their spacing corresponds to the spontaneous wavelength, the adaptation by tip splitting is blocked and an anomalous spacing is forced. Each cell is then affected by dendritic instability. This mimics directional solidification of anisotropic crystals.

¹⁸(a) A. Simon, J. Bechhoefer, and A. Libchaber, *Phys. Rev. Lett.* **61**, 2574 (1988); (b) G. Faivre, S. de Cheveigné, C. Guthmann, and P. Kurowski (to be published).

¹⁹P. Couillet (private communication).

²⁰It is worth noting that these packets of propagating cells have boundaries moving with the cells at the same velocity. They are thus clearly different from the compressive waves observed as transients along the V_1 axis.

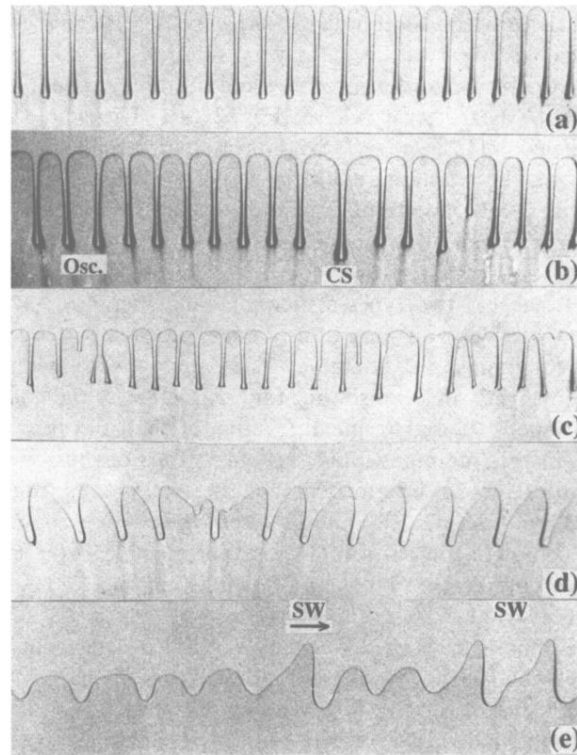


FIG. 2. In a cell with $b_0 = 0.37$ mm, photographs of a part of the front in the cases of (a) a stable pattern of stationary cells; (b) a pattern with weak spatiotemporal chaos showing a coherent structure (CS) and cells oscillating in time (Osc); (c) a pattern with strong spatiotemporal chaos; (d) a pattern of traveling waves, showing a source and a sink; and (e) solitary waves (SW) propagating on a stationary sinusoid.

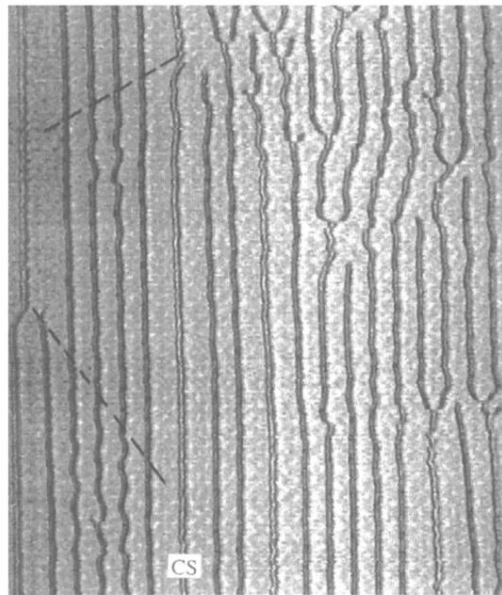


FIG. 3. Spatiotemporal evolution of a part of a front showing weak chaos (each horizontal line is a section of the front so that the dark lines show the positions of the oil films separating the cells) showing the stability of anomalous cells (CS), the coexistence of ordered and disordered regions, and a defect generating oscillations of the cells which propagate (dashed lines). The time elapsed from the top to the bottom is 20 s.